JOURNAL OF AL AZHAR UNIVERSITY ENGINEERING SECTOR
VOL. 3, NO. 9, OCTOBER, 2008, 1034-1046

I.

ACTIVE VIBRATION SUPPRESSION OF A CUTTING TOOL UTILIZING THE FINITE ELEMENT METHOD

Ayman A. El-Badawy
Department of Engineering Mechanics, Faculty of Engineering and Materials Science
The German University in Cairo, New Cairo City, Al-Tagamoa Al Khames, Egypt

الهدف من هذا البحث هو عمل نموذج محاكى لديناميكا أداة القطع ، والمشغلات ذات الخواص البيزوكهربية باستخدام التحليل بالعناصر المحدودة ؛ وكذلك عمل برنامج خاص باستخدام FORTRAN ليعمل بالتوالى مع روتين ثانوي من برنامج ABAQUS وذلك لتطبيق استخدام تحكم من النوع المعروف باسم "التغذية العكسية لإشارة الموقع الموجبة" لإخماد الاهتزازات الناتجة عن عملية القطع.

ABSTRACT
The motivation of the work is to simulate the cutting tool dynamics, the piezoelectric actuators using the finite element method (FEM); Also, developing of a custom made FORTRAN program that is executed in series with the steady-state analysis subroutine in ABAQUS™ to be able to implement positive position feedback (PPF) control law to suppress the vibrations generated during the cutting process.

KEYWORDS: Finite Element, Piezoelectric, Control, Chatter

1. INTRODUCTION
Engineers have used mechanical vibration absorbers (MVAs), or tuned mass dampers, to control vibrating structures for over a century. Basically, a single degree of freedom (DOF) mass-spring system is added to the structure, and tuned to its resonance frequency. When properly tuned, the MVA reduces the response of the system to a narrow band harmonic excitation near the tuning frequency. If a damper is added to the absorber, response to broadband excitation is reduced as well.

The close tolerances of a cutting tool make the use of MVAs impractical. Fortunately, piezoelectric elements provide an alternative that is small, light in weight, and can be bonded directly to the structure. Piezoelectric materials transform strain energy into electrical energy, and vice versa, so they can be used as both sensors and actuators. Forward [1] created a piezoelectric vibration absorber (PVA) using a piezoelectric element and a passive resonant electrical circuit, or shunt which is also analogous to an MVA. The piezoelectric element behaves as a capacitor which is comparable to the spring in an MVA. The shunt is comprised of an inductor (comparable to the mass), and a resistor (comparable to the damper). As the structure vibrates, the piezoelectric element transforms a portion of the strain energy into electrical energy. Tuning the piezoelectric shunt near a structural mode dissipates the electrical energy in the resistor, similar to a tuned mass damper [2]. This coupling between electric potential gradient and strain is the material's piezoelectric property. The material will also have a dielectric property so that an electrical charge exists when the material has a potential gradient.

The concept of position and velocity feedback have been simulated numerically and analyzed experimentally by Paolo Gaudenzi et al [3] to attenuate the vibration effects in active cantilever beam. The numerical simulation has been developed by means of a finite element approach based on Euler-Bernoulli model.

Adachi et al [4] developed a design method of active/passive hybrid type of piezoelectric damping system for reducing the dynamic response of the flexible structures due to external dynamic loads. The designed method was based on the numerical optimization technique whose objective function is a control effort of the active damping. A vibration suppression performance, which is evaluated by the maximum value of the gain of the frequency response function of the structure, is constrained. The used model consists of a three story flexible structure equipped with 12 surface bonded piezoelectric (PZT) tiles pairs.

Optimal piezo-actuator sizes and locations for a frame structure under bending load were presented by Adali et al [5]. The bending moments generated by the piezo-actuators are used for deflection control, i.e., to minimize the maximum deflection. The used frame was subjected to a tip load which lies in an uncertainty domain with regard to its direction.

Shan et al [6] applied the positive position feedback (PPF) controller to the PZT actuators for suppressing multi-mode vibrations while slewing the single-link flexible manipulator. Both set point and trajectory tracking control are considered. Moreover, PPF showed good results than velocity feedback. The hardware experiments verified the proposed method.

However, there are numerous works concerning the active vibration suppression. Of interest is the work by Hu and Ma [7], who investigated the use of variable structure control (VSC) and positive position feedback (PPF) techniques for vibration reduction of flexible spacecraft during attitude maneuver. They used the smart materials as sensors and actuators. The VSC technique is used to suppress large amplitude vibrations excited during rapid maneuvers while the technique of PPF control using PZT as sensors/actuators was implemented for suppression of micro vibrations, i.e., fine tuning the system at the final stage of operations, which is desirable for precision pointing of advanced spacecraft.

In this research, an experimental modal analysis setup has been constructed to investigate the frequency response function (FRF) of the cutting tool. A formulation of the PPF control law utilizing the piezoelectric actuators has been developed. A finite element analysis has been used to simulate the effectiveness of this control scheme in suppressing the tool vibrations during the cutting process.

2. SETUP AND MODAL PROPERTIES

First to model chatter, the values of the natural frequency and damping ratio of the cutting tool for the first transverse vibration mode need to be determined. These dynamic properties were identified using impact testing. A schematic representation of the experimental setup is shown in Figure 1. It consists of a shaper machine, accelerometer, impulse hammer, spectrum analyzer and a PC.

The absolute value of the measured frequency response function is depicted in Figure 2 (mean of 10 measurements). From this frequency response function, the natural frequency and damping ratio of the first bending mode of tool were found to be 1645 Hz and 0.091 respectively.

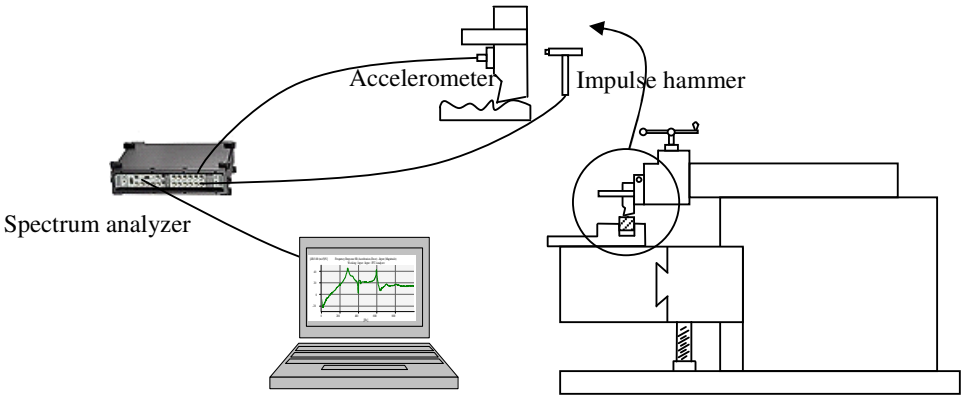

Fig. 1. Shaper machine, workpiece, and data acquisition system layout.

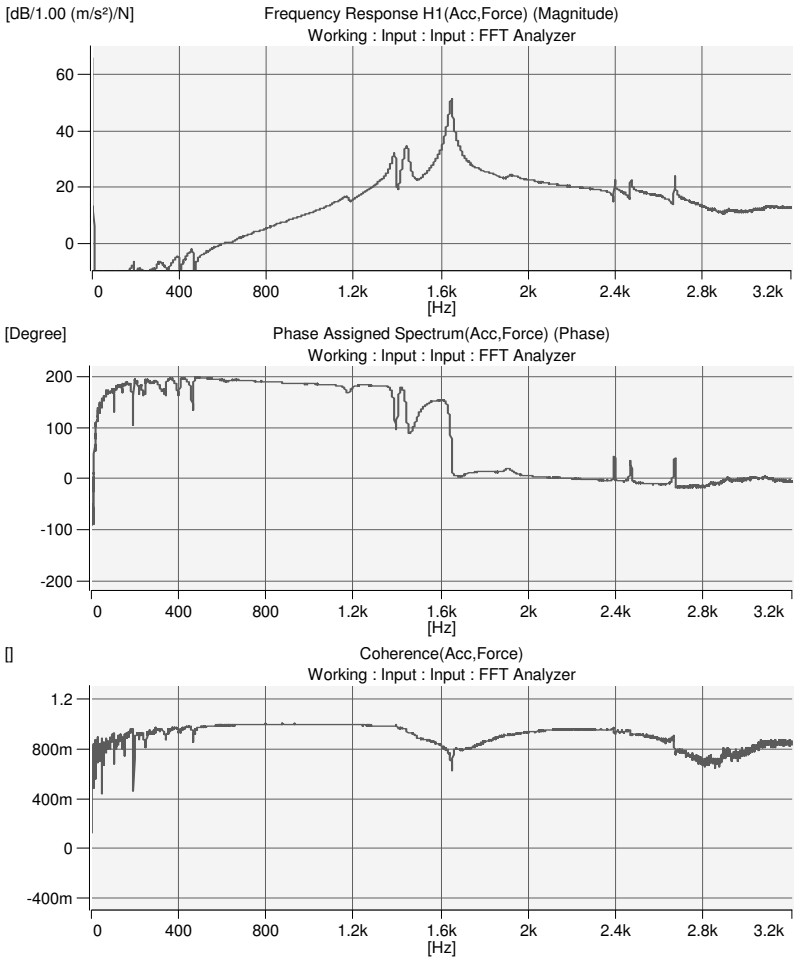

Fig. 2. Frequency response function for the tool (magnitude, phase and coherence).

3. FUNDAMENTALS OF PIEZOELECTRICITY

The constitutive equations describing the piezoelectric property are based on the assumption that the total strain in the transducer is the sum of mechanical strain induced by the mechanical stress and the controllable actuation strain caused by the applied electric voltage. The axes are identified by numerals rather than letters. In Figure 3, 1 refers to the x axis, 2 corresponds to the y axis, and 3 corresponds to the z axis. Axis 3 is assigned to the direction of the initial polarization of the piezoceramic, and axes 1 and 2 lie in the plane perpendicular to axis 3.

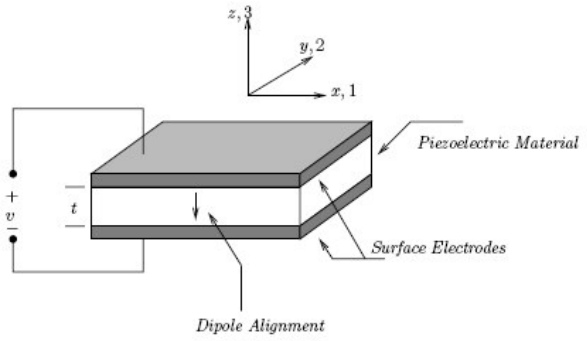

Fig. 3. Schematic diagram of a piezoelectric transducer [8].

The describing electromechanical equations for a linear piezoelectric material can be written as [9]:

$$\varepsilon_i = S_{ij}^E \sigma_j + d_{mi} E_m \tag{5.1}$$

$$D_m = d_{mi} \sigma_i + \xi_{ik}^\sigma E_k \tag{5.2}$$

Where the indices $i, j = 1, 2\ldots, 6$ and $m, k = 1, 2, 3$ refer to different directions within the material coordinate system. The above equations can be re-written in the following form, which is often used for applications that involve sensing:

$$\varepsilon_i = S_{ij}^D \sigma_j + g_{mi} D_m \tag{5.3}$$

$$E_i = g_{mi} \sigma_i + \beta_{ik}^\sigma D_k \tag{5.4}$$

Where

σ: stress vector (N/m^2)

ε: strain vector (m/m)

E: vector of applied electric field (V/m)

ξ: permitivity (F/m)

d: matrix of piezoelectric strain constants (m/V)

S: matrix of compliance coefficients (m^2/N)

D: vector of electric displacement (C/m^2)

g: matrix of piezoelectric constants (m^2/C)

β: impermitivity (m/F)

Furthermore, the superscripts D, E, and σ represent measurements taken at constant electric displacement, constant electric field and constant stress respectively.

Equations (5.1) and (5.3) express the converse piezoelectric effect, which describes the situation when the device is being used as an actuator. Equations (5.2) and (5.4), on the other hand, express the direct piezoelectric effect, which deals with the case when the transducer is being used as a sensor. The converse effect is often used to determine the piezoelectric coefficients.
In matrix form, equations (5.1)-(5.4) can be written as:

$$\begin{bmatrix} \varepsilon_1 \\ \vdots \\ \varepsilon_6 \end{bmatrix} = \begin{bmatrix} S_{11} & \cdots & S_{16} \\ \vdots & \ddots & \vdots \\ S_{61} & \cdots & S_{66} \end{bmatrix} \begin{bmatrix} \sigma_1 \\ \sigma_2 \\ \sigma_3 \\ \tau_{23} \\ \tau_{31} \\ \tau_{12} \end{bmatrix} + \begin{bmatrix} d_{11} & d_{21} & d_{31} \\ \vdots & \vdots & \vdots \\ d_{16} & d_{26} & d_{36} \end{bmatrix} \begin{bmatrix} E_1 \\ E_2 \\ E_3 \end{bmatrix} \tag{5.5}$$

$$\begin{bmatrix} D_1 \\ D_2 \\ D_3 \end{bmatrix} = \begin{bmatrix} d_{11} & \cdots & d_{16} \\ d_{21} & \cdots & d_{26} \\ d_{31} & \cdots & d_{36} \end{bmatrix} \begin{bmatrix} \sigma_1 \\ \sigma_2 \\ \sigma_3 \\ \sigma_{23} \\ \sigma_{31} \\ \sigma_{12} \end{bmatrix} + \begin{bmatrix} e_{11}^{\sigma} & e_{12}^{\sigma} & e_{13}^{\sigma} \\ e_{21}^{\sigma} & e_{22}^{\sigma} & e_{23}^{\sigma} \\ e_{31}^{\sigma} & e_{32}^{\sigma} & e_{33}^{\sigma} \end{bmatrix} \begin{bmatrix} E_1 \\ E_2 \\ E_3 \end{bmatrix} \tag{5.6}$$

Assuming that the device is poled along axis 3, and viewing the piezoelectric material as a transversely isotropic material, which is true for piezoelectric ceramics, many of the parameters in the above matrices will be either zero, or can be expressed in terms of other parameters. In particular, the non-zero compliance coefficients are:

$$S_{11} = S_{22}\ ,\ S_{13} = S_{31} = S_{23} = S_{32}$$
$$S_{12} = S_{21}\ ,\ S_{44} = S_{55}\ ,\ S_{66} = 2(S_{11} - S_{12})$$

The non-zero piezoelectric strain constants are

$$d_{31} = d_{32}\ ,\ d_{15} = d_{24}$$

Finally, the non-zero dielectric coefficients are $e_{11}^{\sigma} = e_{22}^{\sigma}$ and e_{33}^{σ} . Subsequently the equations (5.5) and (5.6) are simplified to:

$$\begin{bmatrix}\varepsilon_1\\ \varepsilon_2\\ \varepsilon_3\\ \varepsilon_4\\ \varepsilon_5\\ \varepsilon_6\end{bmatrix}=\begin{bmatrix}S_{11} & S_{12} & S_{13} & 0 & 0 & 0\\ S_{12} & S_{11} & S_{13} & 0 & 0 & 0\\ S_{13} & S_{13} & S_{33} & 0 & 0 & 0\\ 0 & 0 & 0 & S_{44} & 0 & 0\\ 0 & 0 & 0 & 0 & S_{44} & 0\\ 0 & 0 & 0 & 0 & 0 & 2(S_{11}-S_{12})\end{bmatrix}\begin{bmatrix}\sigma_1\\ \sigma_2\\ \sigma_3\\ \tau_{23}\\ \tau_{31}\\ \tau_{12}\end{bmatrix}+\begin{bmatrix}0 & 0 & d_{31}\\ 0 & 0 & d_{31}\\ 0 & 0 & d_{33}\\ 0 & d_{15} & d_{34}\\ d_{15} & 0 & 0\\ 0 & 0 & 0\end{bmatrix}\begin{bmatrix}E_1\\ E_2\\ E_3\end{bmatrix} \tag{5.7}$$

$$\begin{bmatrix}D_1\\ D_2\\ D_3\end{bmatrix}=\begin{bmatrix}0 & 0 & 0 & 0 & d_{15} & 0\\ 0 & 0 & 0 & d_{15} & 0 & 0\\ d_{31} & d_{31} & d_{33} & 0 & 0 & 0\end{bmatrix}\begin{bmatrix}\sigma_1\\ \sigma_2\\ \sigma_3\\ \sigma_{23}\\ \sigma_{31}\\ \sigma_{12}\end{bmatrix}+\begin{bmatrix}e_{11}^{\sigma} & 0 & 0\\ 0 & e_{22}^{\sigma} & 0\\ 0 & 0 & e_{33}^{\sigma}\end{bmatrix}\begin{bmatrix}E_1\\ E_2\\ E_3\end{bmatrix} \tag{5.8}$$

Consider a beam with a pair of collocated piezoelectric transducers bonded to it as shown in Figure 4. The purpose of actuators is to generate bending in the beam by applying a moment to it. This is done by applying equal voltages, of 180° phase difference, to the two patches. Therefore, when one patch expands, the other contracts. Due to the phase difference between the voltages applied to the two actuators, only pure bending of the beam will occur.

When a voltage V is applied to one of the piezoelectric elements, in the direction of the polarization vector, the actuator strains in direction 1 (the x-axis). Furthermore, the amount of free strain is given by:

$$\varepsilon_p = \frac{d_{31}V}{t_p}$$

where t_p represents the thickness of the piezoelectric actuator.

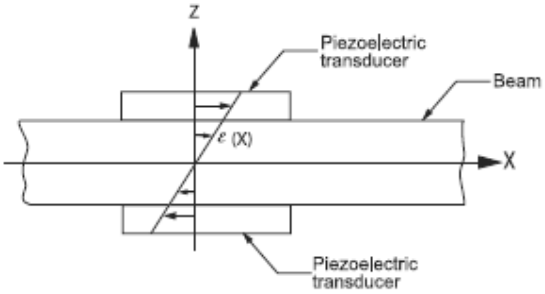

Fig. 4. A beam with a pair of identical collocated piezoelectric actuators.

4. FINITE ELEMENT MODELING

A three dimensional Cartesian coordinate system is used. The cutting tool of extent length L in the x_2-direction and $b*b$ in the x_1 and x_3-directions. The tool is fixed at one end and free at the other end, as shown in Figure 5.

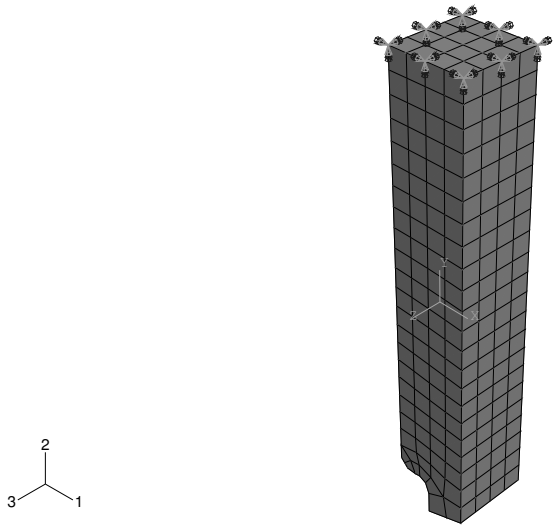

Fig. 5. Three dimensional Cartesian coordinate for the used tool.

A three dimensional finite element model of machine tool structure has been developed using ABAQUS® software. To validate the FE model, the natural frequency results will be compared with those obtained by mathematical calculations and experimental verifications.

The element used in analysis is C3D8R. The C3D8R is a general 3D 8-node, linear brick plane strain element with reduced integration. Plain strain deals with a situation in which the dimension of the structure in one direction (x_2) is large in comparison with the dimensions of the structure in the other two directions (x_1 and x_3 directions).

A mesh convergence study is performed to ensure that the finite element model produces solutions that have converged to an acceptable limit. The natural frequency of the system without the actuator is used as the convergence criterion. The results of this study can be found in figure 6 as a plot of the number of elements in the mesh versus the natural frequency.

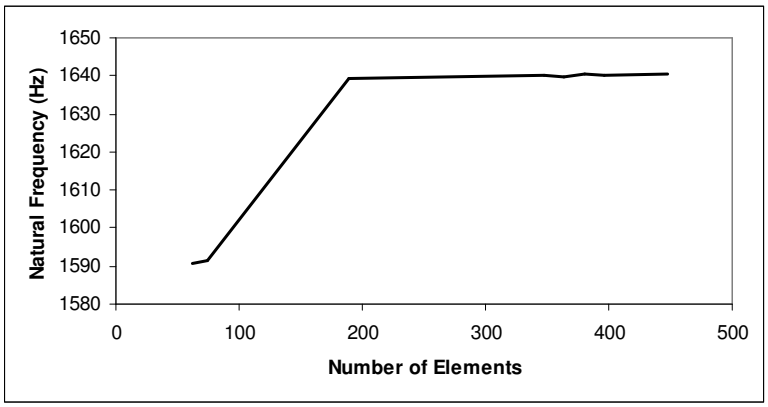

Fig. 6. A convergence study of the natural frequency of the cutting tool.

As can be seen from Figure 6, the solution has converged when the number of elements in the mesh reaches 189 elements. 364 elements and 600 nodes are used to model the cantilever tool. The resulting mesh for the tool is used in all of the finite element analyses.

The natural frequency of the tool is extracted using the Lanczos method. The other method offered by ABAQUS® is a subspace iteration Eigen-value extraction. The Lanczos method is preferred in this instance because it is typically faster. The results of the mathematical solution [10], experimental results and FEA are typically compared in Table 1. The natural frequency and mode shape are the result of a free vibration analysis. System identification is very important to any vibration suppression control scheme. Once the natural frequency and mode shape are known, vibration suppression using Positive Position Feedback "PPF" is undertaken to determine the influence of the control parameters on the system damping. The mode shape corresponding to the first natural frequency is depicted in Figure 7.

Table 1. The extracted FE natural frequency of the tool compared with the mathematical and experimental solutions.

Mode	Mathematical (Hz)	Experimental (Hz)	Finite Element (Hz)
ω_1	1598	1645	1640.3

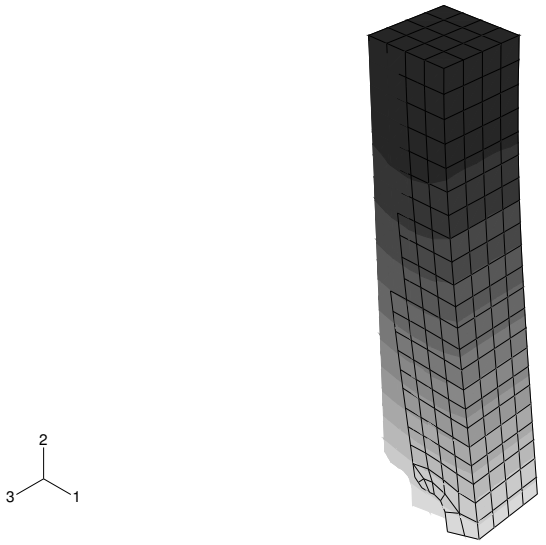

Fig. 7. First mode shape corresponding to the first natural frequency of the tool .

5. POSITIVE POSITION FEEDBACK CONTROL LAW

The system shown in Figure 8 is a closed-loop feedback control system since the signal sent to the actuator is a direct result of the incoming sensor signal. The process of active vibration control happens as follows: a sensory signal from the excited structure is detected by the control system, the signal is processed by a control algorithm and an appropriate signal is sent to the actuator. An important part of the control scheme is the control algorithm because this determines how the structure responds to external excitation sources.

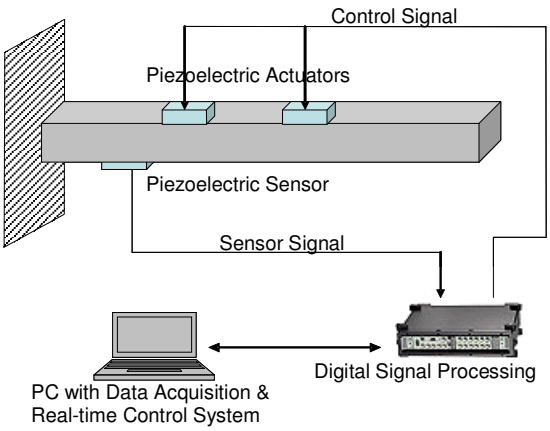

Fig. 8. Feedback vibration suppression control scheme using piezoelectric elements.

A control algorithm that actively dampens vibrations is a method called positive position feedback (PPF), which was first noted by Goh and Caughey [11]. The PPF control uses second order differential equations to model the interaction between the system and compensator. The advantage of this system is that individual modes can be targeted for active vibration suppression.

The structure/compensator interaction is as follows [12].

The structure $$\ddot{u} + 2\zeta\omega_n\dot{u} + \omega_n^2 u = g\,\omega_c^2\eta \tag{5.9}$$

The compensator $$\ddot{\eta} + 2\zeta_c\omega_c\dot{\eta} + \omega_c^2\eta = \omega_c^2 u \tag{5.10}$$

where u is the modal coordinate, η is the compensator coordinate, ζ is damping ratio of the structure, ω_n is the natural frequency of the structure, ζ_c is the compensator damping ratio, ω_c is the compensator frequency and g is a scalar gain. Figure 9 illustrates the connection of structure/compensator equations in a block diagram.

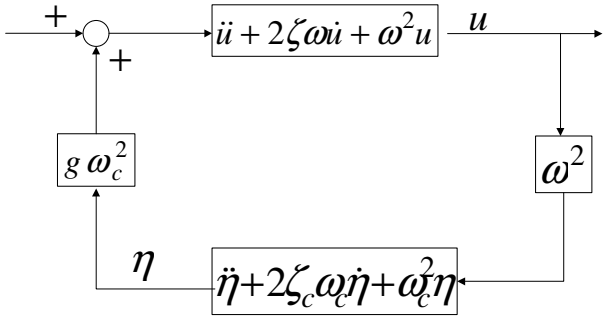

Fig. 9. Block diagram of a second-order system with positive position feedback .

As we can see from the structure/compensator equations, there are three quantities that must be appropriately chosen to implement this feedback control. These quantities are the scalar gain g, the compensator natural frequency ω_c and the compensator damping ratio ζ_c. The rest of the quantities are a direct result of the physical system. The scalar gain must lie within the range of $0 < g < 1$ for stability [13]. The range for the compensator damping ratio found in the literature reaches from ζ_c = 0.01 to 0.5. Most authors suggest a value for the compensator frequency ω_c slightly greater than the structural frequency to be damped. While Dosch, et al [14] specified a factor of 1.3 between ω_n and ω_c, Fagan [15] chooses 1.45.

For steady-state vibration $\eta = \eta_0 e^{i\omega t}$ and $u_1 = u_1^0 e^{i\omega t}$. Therefore, (5.10) becomes:

$$-\omega^2\eta_0 + 2i\omega_c\omega\eta_0 + \omega_c^2\eta_0 = \omega_c^2 u_1^0 \tag{5.11}$$

Solving for η_0:

$$\eta_0 = \left[\frac{\omega_c^2}{\left(\omega_c^2 - \omega^2\right) + 2i\omega_c\omega}\right] u_1^0 \tag{5.12}$$

The applied feedback potential to the piezoelectric actuator is as follows:

$$\phi_0 = g\omega_c^2\eta_0 \tag{5.13}$$

where *g* is the feedback gain.
The following potential is applied to the actuator to suppress the vibration:

$$\phi = \phi_0 e^{i\omega t} \tag{5.14}$$

6. FINITE ELEMENT ANALYSIS

The natural frequencies of the combined model "tool and piezoelectric actuators" are also computed by the finite element method using the commercial finite element package ABAQUS/Standard 6.6-3®. Table 2 shows the new combined model modal frequencies compared with tool's original modal frequency.

Table 2. The Modal frequencies of the tool compared with the combined model

	Modal Frequency (Hz)	
Tool	1640.30	
New combined model	1580.83	2147.00

The elements used in the analysis are C3D8R and C3D8E for the tool and piezoelectric materials respectively. The C3D8R is 8-node linear brick, reduced integration stress/displacement element. The C3D8E is 8-node linear brick piezoelectric element. The number of elements and nodes for all the finite element studies were kept constant at 564 elements and 1,004 nodes. The ABAQUS simulation of the piezoelectric actuator properties which satisfy the second order system are defined by the density, modulus of elasticity, material damping, piezoelectric strain constants, dielectric constant and boundary conditions.

The second implemented analysis was the frequency response of the system which is computed using DIRECT, STEADY STATE subroutine. This includes both the uncontrolled and actively controlled response of the cutting tool.

The frequency response function of the uncontrolled system is determined by computing the steady-state response of the tool to an applied force which is integrated from the measured acceleration data shown in figure 10.

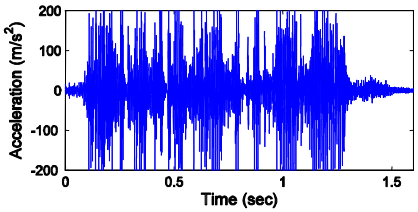

Fig. 10. Time trace of the tool acceleration for *DOC*=0.70mm and 12 strokes/min cutting speed.

Computing the frequency response curve of the cutting tool with feedback control required the development of a custom made FORTRAN program that is executed in series with the steady-state analysis subroutine in ABAQUS®. An arbitrary complex voltage is applied to the control actuator as an initial value. A steady-state finite element solution is obtained using this assumed electric potential. The strain near the root of the tool is obtained from the finite element solution and the corresponding steady-state feedback control voltage is computed based on the PPF control law. The computed value of control potential is compared with the assumed potential. The analysis procedure is iterated until the difference between the prescribed potential and calculated control potential is zero. This is accomplished by defining a complex function, which calculates the difference between the computed and assumed control voltages. The complex zero of the analytic function is obtained using the secant method of root finding using quadratic 3-point interpolation. The obtained root is the voltage applied to the control actuator which satisfies the PPF feedback control law. The process is repeated for several frequency values to create a frequency response curve.

7. RESULTS AND DISCUSSION

Parametric study is performed to quantify the effect of PPF controller damping ratio on system damping. The base compensator utilized in the parametric study consisted of a controller frequency ω_c that is 1.219 times the fundamental frequency (ω_n= 1640.3 Hz). Three different controller damping ratios of ζ_c = 0.01, 0.1 and 0.5 are studied. The frequency response curves and corresponding phase plots are shown in Figure 11.

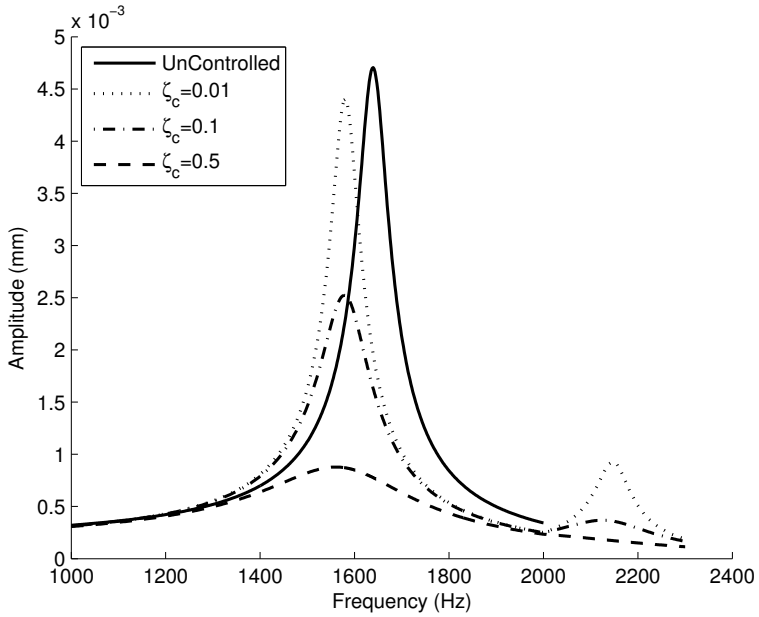

Fig. 11. Frequency response and phase plots for (Uncontrolled, ζ_c = 0.01, ζ_c = 0.1 and ζ_c = 0.5).

As can be seen from Figure 11 a significant reduction in peak responses occur while increasing the compensator damping ratio from 0.01 to 0.1 compared to in case of absence of active feedback control. While increasing the damping ratio to 0.5 the system behaves as a single degree of freedom system; the two systems – tool and actuators – are virtually clamped together.

Figure 12a and b show the peak amplitude along the tool length in a normalized distance for both positions (front and back edges of the tool). The influence of the compensator damping is as expected. System damping increases as the compensator damping is increased.

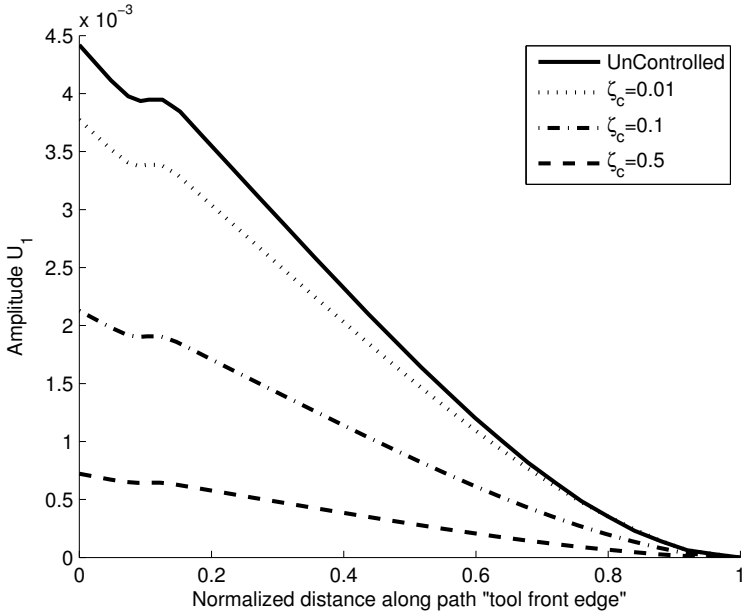

(a)

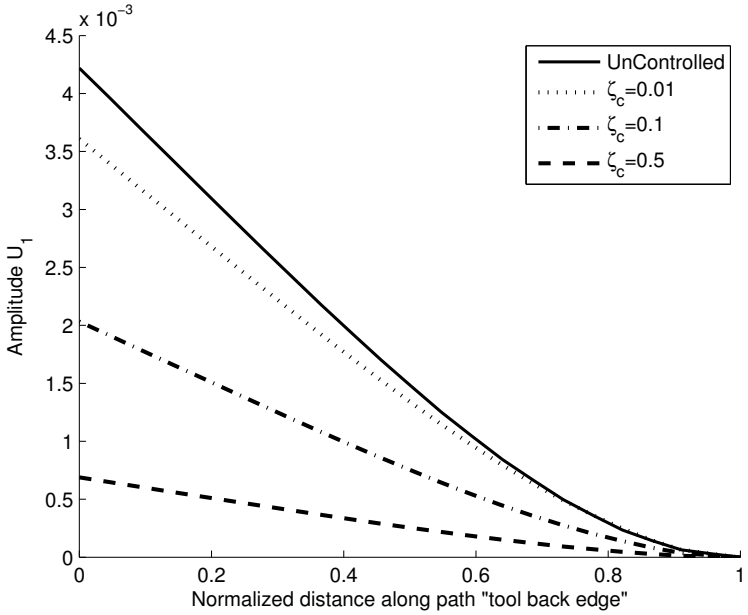

(b)

Fig. 12. Peak amplitude along the length of the tool (a: Front edge, b: Back edge).

8. CONCLUSIONS

An active vibration suppression of a machine-tool with embedded piezoelectric actuators and sensors is presented. A finite element investigation utilizing the positive position feedback (PPF) control laws is used for active vibration suppression. The finite element analyses are performed using the commercial finite element package ABAQUS/Standard 6.6-3®. It is found that utilizing the FEA with piezoelectric actuators is a viable option when developing active vibration suppression systems.

REFERENCES

1. Forward, Robert L. "Electronic Damping of Vibrations in Optical Structures," *Applied Optics*, Vol. 18, No. 5, 1979, pp. 690–697.
2. Agnes, Gregory S. and Daniel J. Inman. "Nonlinear Piezoelectric Vibration Absorbers," *Smart Material Structures*, Vol. 5, 1996, pp.704–714.
3. P. Gaudenzi, R. Carobonaro, E. Benzi, "Control of Beam vibrations by means of Piezoelectric Devices: Theory and Experiments", *Composite Structures*, Vol. 50, 2000, pp. 373-379.
4. K. Adachi, Y. Kitamura, T. Iwatsubo, "Integrated Design of Piezoelectric Damping System for Flexible Structure", *Applied Acoustics*, Vol.65, 2004, pp. 293-310.
5. S. Adali, I. S. Sadek, J. C. Bruch Jr, J. M. Sloss, I. U. Cagdas, "Optimal Sizing of Piezo-actuators for Minimum Deflection Design of Frames under Uncertain Loads", *Journal of The Franklin Institute*, Article in press
6. J. Shan, H. Liu, D. Sun, "Slewing and Vibration Control of a Single-link Flexible Manipulator by Positive Position Feedback (PPF)", *Mechatronisc*, Vol. 15, 2005, pp. 487-503.
7. Q. Hu, G. Ma, "Variable Structure Control and Active Vibration Suppression of Flexible Spacecraft during Attitude Maneuver", *Aerospace Science and Technology*, Vol. 9, 2005, pp. 307-317.
8. Reza Moheimani, Andrew Fleming, *Piezoelectric Transducers for Vibration Control and Damping*, Springer-Verlag, London, 2006.
9. Institute of Electrical Engineers Inc. IEEE standard on piezoelectricity. ANSI/IEEE Std. 176-1987, 1988.
10. S. S. Rao, *Mechanical Vibrations*, Pearson Prentice Hall, 2004.
11. C. J. Goh and T. K. Caughey. "On the Stability Problem Caused by Finite Actuator Dynamics in the Collocated Control of Large Space Structures," *International Journal of Control*, Vol. 41, No. 3, 1985, pp.787-802.
12. M. I. Friswell and D. J. Inman. "The Relationship between Positive Position Feedback and Output Feedback Controllers," *Smart Materials and Structures*, Vol. 8, 1999, pp.285-291.
13. J. L. Fanson and T. K. Caughey. "Positive Position Feedback Control for Large Space Structures," *AIAA Journal*, Vol. 28, No. 4, 1990, pp.717-724.
14. J. J. Dosch, D. J. Inman, E. Garcia. "A Self-Sensing Piezoelectric Actuator for Collocated Control," *Journal of Intelligent Material Systems and Structures*, Vol. 3, 1992.
15. G. T. Fagan. "An Experimental Investigation into Active Damage Control Systems Using Positive Position Feedback for AVC", *Master Thesis, Virginia Tech*, 1993.